Supporting information

Shape Transformation of {*hk*0}-faceted Pt Nanocrystals from Tetrahexahedron to Truncated Ditetragonal Prism

Jia-Huan Du, Tian Sheng, Chi Xiao, Na Tian*, Jing Xiao, Ai-Yun Xie, Shuo Liu, Zhi-You Zhou, Shi-Gang Sun*

Email: tnsd@xmu.edu.cn; sgsun@xmu.edu.cn

State Key Laboratory of Physical Chemistry of Solid Surfaces, Collaborative Innovation Center of Chemistry for Energy Materials, College of Chemistry and Chemical Engineering, Xiamen University, Xiamen 361005, China

1. Materials and methods

H_2PtCl_6 (99.99%) was purchased from Alfa Aesar. Sulfuric acid (G.R. reagent) was purchased from China Medicine Shanghai Chemical Reagent Corp. All chemicals were used as received. The solutions were prepared from super pure water (18 MΩ cm) purified through a Milli-Q Lab system (Nihon Millipore Ltd.).

Electrochemical preparation of Pt nanocrystals was carried out in a standard three-electrode cell at room temperature. The working electrode was a polished glassy carbon (GC, ϕ = 6 mm) electrode. The counter electrode was a Pt foil and reference electrode was a saturated calomel electrode (SCE). All potentials reported in this paper are referred to the SCE scale. Electrode potential was controlled by PAR 263A potentiostat/galvanostat (EG&G) via a home-developed software that can realize arbitrary potential waveform function as required.
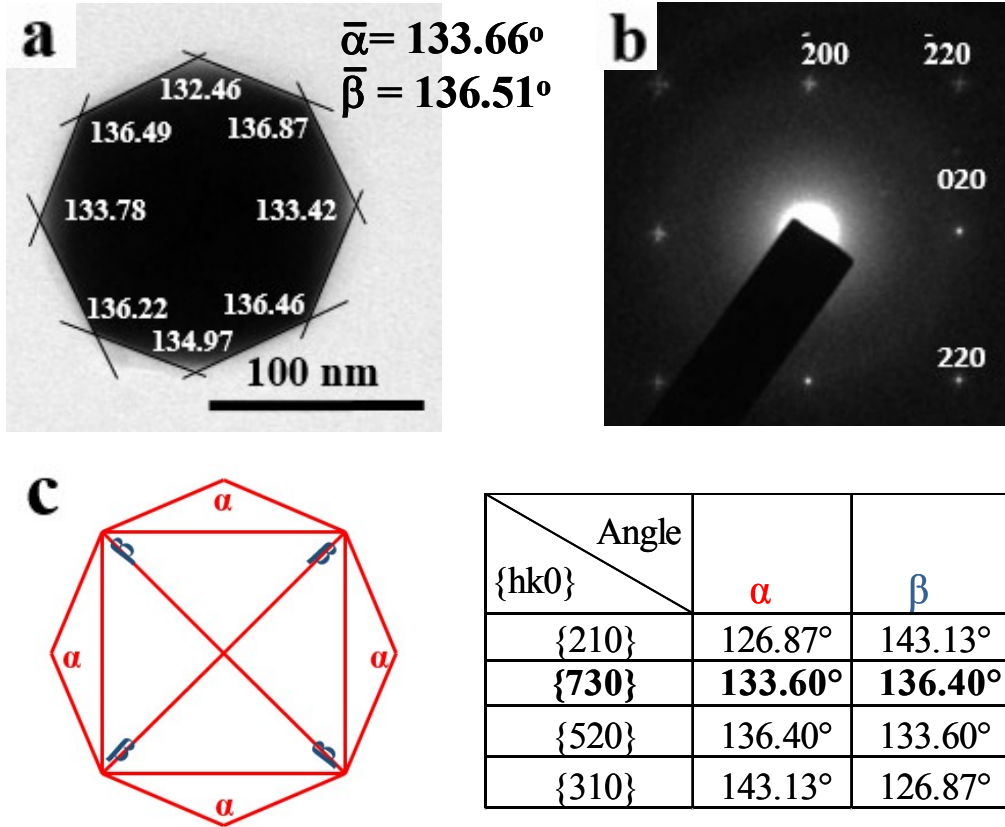
Tetrahexahedral Pt nanocrystals (THH Pt NCs) were deposited on the GC electrode in 2 mM H_2PtCl_6 + 0.1 M H_2SO_4 solution by programmed potential steps. The potential was stepped from 1.20 to −0.23 V and held for 140 ms to form crystal nuclei. The growth of the crystal nuclei into THH Pt NCs was mediated by electrochemical square-wave potential (SWP) for 20 min. The lower (E_L) and upper (E_U) potential limits were 0.10 and 1.00 V, respectively, and the frequency was 100 Hz. The obtained THH Pt NCs were subjected to the SWP treatment for another 20 min to transform into truncated ditetragonal prism (TDP) in the same solution but at slightly different potentials (E_L = 0.08 V and E_U = 1.15 V). When E_L varied from 0.08 to 0.11 V, TDP Pt NCs can still be obtained.

2. Size distribution of THH Pt NCs
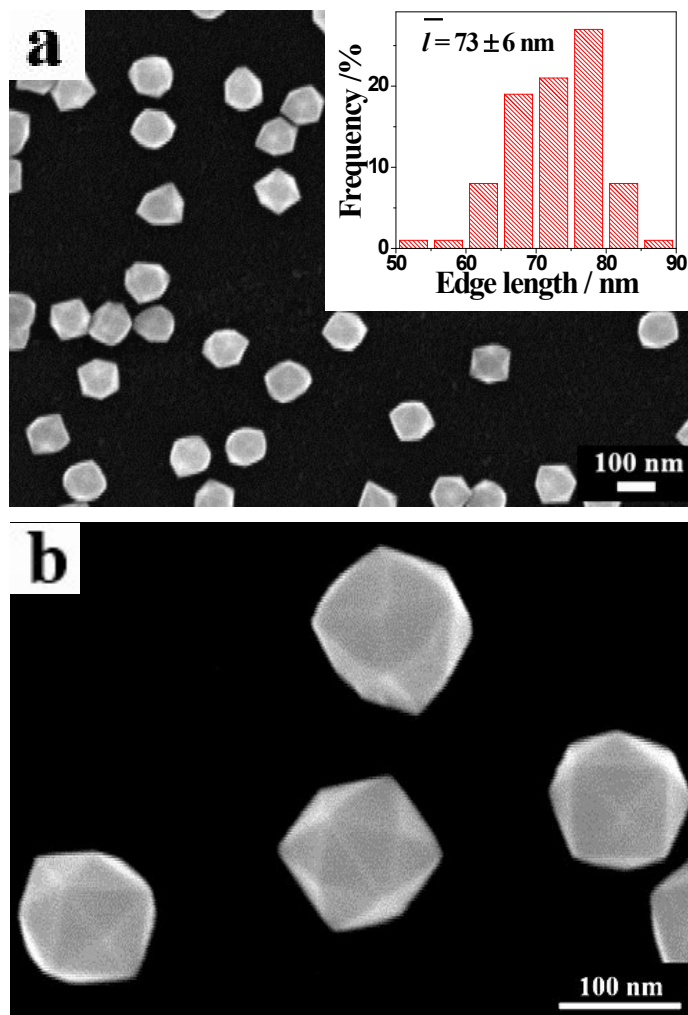
Fig. S1 (a) Low- and (b) high-magnification SEM images of THH Pt NCs obtained at E_L = 0.10 V and E_U = 1.00 V for 20 min in 2 mM H_2PtCl_6 + 0.1 M H_2SO_4 solution. Inset is the size (edge length) histogram. The average cuboid edge length of the THH Pt NCs is 73 nm.

3. Surface structure of THH Pt NCs

a $\bar{\alpha}= 133.66^o$ $\bar{\bar{\beta}} = 136.51^o$

132.46
136.49   136.87
133.78   133.42
136.22   136.46
134.97
100 nm

b $\bar{2}00$ $\bar{2}20$
020
$\bar{2}20$

c

| Angle {hk0}	α	β
{210}	126.87°	143.13°
{730}	**133.60°**	**136.40°**
{520}	136.40°	133.60°
{310}	143.13°	126.87°

Fig. S2 (a) TEM image and (b) SAED pattern of a THH Pt NC along the [001] direction. (c) Theoretical interfacial angles of a THH bounded by different {hk0} facets.
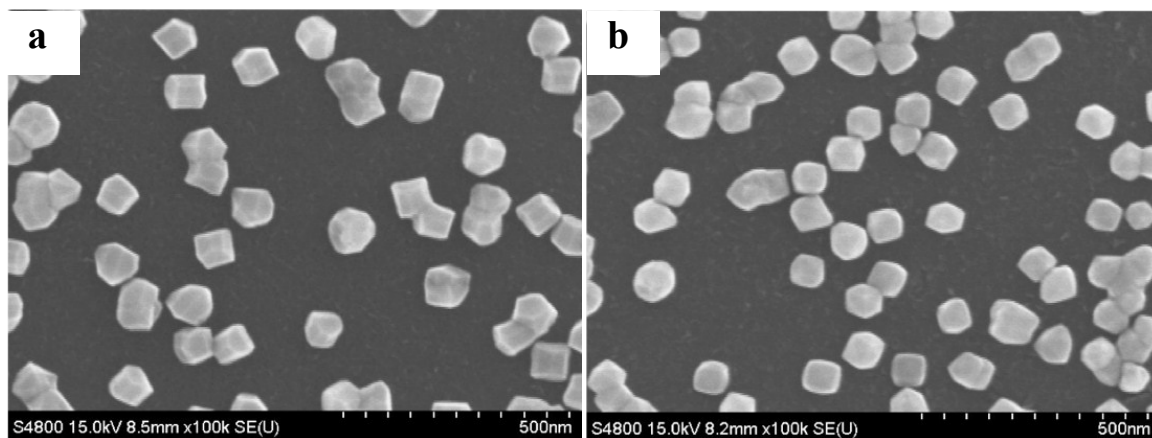
4. Catalytic activity of TDP Pt NCs and THH Pt NCs
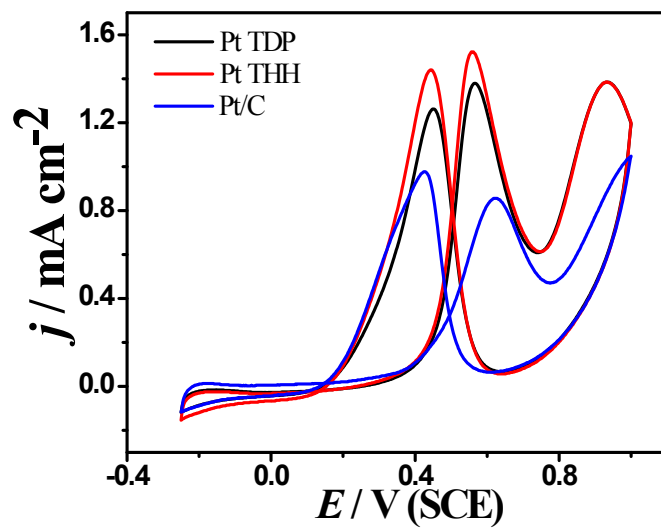
Fig. S3 Cyclic voltammograms of TDP Pt NCs, THH Pt NCs and commercial Pt/C catalysts, at 50 mV s^{-1} in 0.1 M ethanol + 0.1 M HClO$_4$.

5. Effect of E_U and concertration of H_2PtCl_6 on the shape transformation
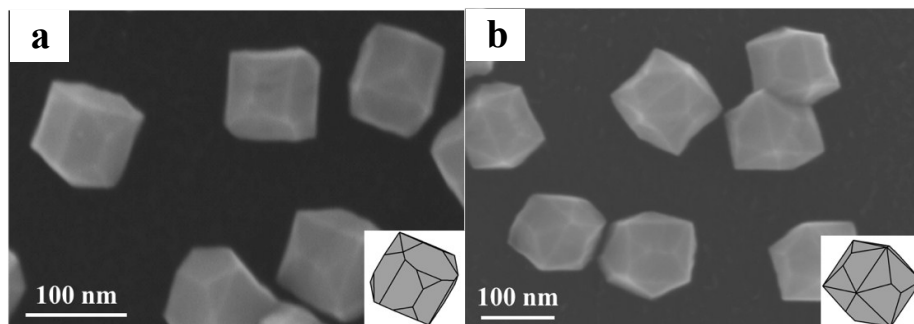
Fig. S4 SEM images of THH Pt NCs treated with decreased E_U of the SWP, while keep E_L unchanged. (a) $E_U = 1.10$ V, (b) $E_U = 1.05$ V.

Fig. S5 SEM images of Pt NCs obtained by SWP treatment of THH Pt NCs under the same experimental parameters as that for the preparation of TDP NCs except that the concertration of H_2PtCl_6 was changed from 2 mM to (a) 1 mM, (b) 0 mM.

6. Computational method

All the electronic structure calculations were performed using the Vienna Ab-initio Simulation Package (VASP) with the exchange-correlation functional of Perdew-Burke-Ernzerh (PBE). The projector-augmented-wave (PAW) pseudopotentials were utilized to describe the core electron interaction.[S1-S9] The perfect vertices of the THH square-based pyramid was modelled with 348 Pt atoms as shown in Fig. S6a and the etching structure was modelled with 399 Pt atoms as shown in Fig. S6b. All the atoms were fixed in their bulk positions in the calculation of the surface energy. The cut-off energy was 400 eV and a 1x1x1 Monkhorst-Pack k-point sampling was used. Models (a) and (b) were modelled based on a $p(7\sqrt{2}$x$7\sqrt{2})$ unit cell with 6-layer Pt and the structure of vertices of the THH square-based pyramid were manually built via the removal of some surface atoms. In the calculation of Pt(100) surface energy, a $p(3$x$3)$ unit cell was used with 4-layer including 36 Pt atoms, and a 3x3x1 Monkhorst-Pack k-point sampling was used. The vacuum region was ~12 Å to ensure that there is little interaction between slabs. The surface energy of Pt(100) (γ_{100}, J m^{-2}) was calculated according to the Eq. (1).

$$\gamma_{100} = (E_{total} - nE_{bulk})/2A_{100} \quad (1)$$

where E_{total} (J) is the total energy of the unit cell, E_{bulk} is the energy of per Pt atom at the bulk position, A_{100} is the surface area (m^2) of Pt(100) surface and n is the number of Pt atoms in the slab. The surface energy of vertices of the THH square-based pyramid (γ_{model}, J m^{-2}) is calculated as the Eq. (2).

$$\gamma_{model} = (E_{total} - A_{100}\gamma_{100} - nE_{bulk})/A_{model} \quad (2)$$

where E_{total} is the total energy of the model. A_{100} is the bottom exposed Pt(100) surface area of slabs, 7.74×10^{-18} m^2. $A_{100}\gamma_{100}$ is the contribution from Pt(100) to the total energy which should be excluded. A_{model} is the surface area, highlighted by the yellow line in Fig. S6, A_{model} is calculated to be 8.43×10^{-18} m^2 in both models (a) and (b). n is the number of Pt atoms used in the model.
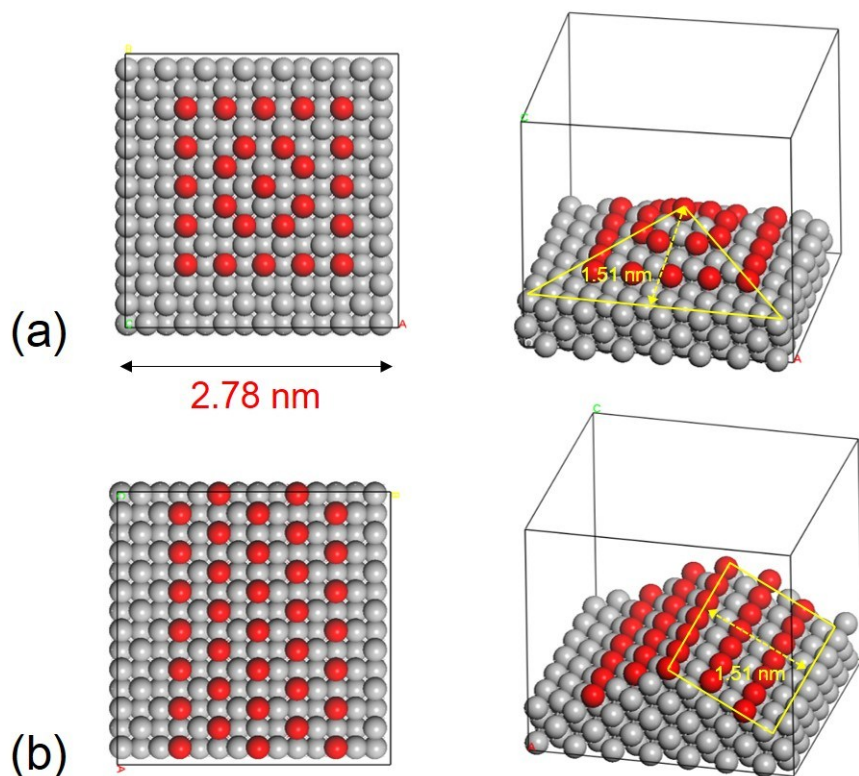
Fig. S6 Models of the vertices of the THH square-based pyramid (a) perfect structure (b) etched structure. Grey: Pt, red: step Pt.

References

S1. Kresse, G.; Hafner, J. *Phys. Rev. B.,* 1993, **48**, 13115.

S2. Kresse, G.; Furthmuler, J. *Phys. Rev. B.,* 1996, **54**, 11169.

S3. Kresse, G.; Hafner, J. *Phys. Rev. B.,* 1993, **47**, 558.

S4. Kresse, G.; Hafner, J., *Phys. Rev. B.,* 1994, **49**, 14251.

S5. Kresse, G.; Furthmuller, J. *Comput. Mater. Sci.,* 1996, **6**, 15.

S6. Blochl, P. E. *Phys. Rev. B.,* 1994, **50**, 17953.

S7. Kresse, G.; Joubert, D. *Phys. Rev. B.,* 1999, **59**, 1758.

S8. Pedrew, J. P.; Burke, K. *Phys. Rev. Lett.,* 1996, **77**, 3865.

S9. Pedrew, J. P.; Burke, K.; Ernzerhof, M. *Phys. Rev. Lett.,* 1997, **78**, 1396.